Helium-Iron Compounds at Terapascal Pressures

Bartomeu Monserrat,[1,2,*] Miguel Martinez-Canales,[3,4] Richard J. Needs,[2] and Chris J. Pickard[5,6]

[1]*Department of Physics and Astronomy, Rutgers University, Piscataway, New Jersey 08854-8019, USA*
[2]*TCM Group, Cavendish Laboratory, University of Cambridge, J. J. Thomson Avenue, Cambridge CB3 0HE, United Kingdom*
[3]*Scottish Universities Physics Alliance, School of Physics and Astronomy, The University of Edinburgh,
Edinburgh EH9 3FD, United Kingdom*
[4]*Centre for Science at Extreme Conditions, The University of Edinburgh, Edinburgh EH9 3FD, United Kingdom*
[5]*Department of Materials Science and Metallurgy, University of Cambridge,
27 Charles Babbage Road, Cambridge CB3 0FS, United Kingdom*
[6]*Advanced Institute for Materials Research, Tohoku University 2-1-1 Katahira, Aoba, Sendai 980-8577, Japan*

We investigate the binary phase diagram of helium and iron using first-principles calculations. We find that helium, which is a noble gas and inert at ambient conditions, forms stable crystalline compounds with iron at terapascal pressures. A FeHe compound becomes stable above 4 TPa, and a $FeHe_2$ compound above 12 TPa. Melting is investigated using molecular dynamics simulations, and a superionic phase with sublattice melting of the helium atoms is predicted. We discuss the implications of our predicted helium-iron phase diagram for interiors of giant (exo)planets and white dwarf stars.

Matter under extreme compression exhibits rich and unexpected behavior, such as unconventional chemistry [1,2], structure [3], and phases [4]. Inside planets and stars, electrons and nuclei are subject to extreme conditions of pressure and temperature, and the exploration of new physics and chemistry under these conditions is necessary for the study of astrophysical processes within the interior of Earth [5–7], other planets [8,9], or stars [10–12].

Static experiments using diamond anvil cells have reached pressures of one terapascal (TPa, 1 TPa = 10^7 atmospheres) [13], well above those at the center of Earth but smaller than those found at the cores of giant gas planets such as Jupiter and Saturn [14]. Higher pressures can be explored with dynamic compression experiments, as exemplified by the recent report from a team in the U.S. National Ignition Facility that subjected diamond to pressures of 5 TPa [15,16]. With high-pressure experiments starting to investigate the realm of terapascal physics and chemistry, theoretical predictions are starting to emerge that reveal unexpected behavior and complexity under these conditions.

In this context, we use quantum mechanical calculations to explore the phase diagram of helium and iron, two of the most abundant elements in the Universe.

Helium nuclei formed in the early Universe during big bang nucleosynthesis, and the primordial 25% mass fraction of helium makes it the second most abundant element after hydrogen. In addition, thermonuclear reactions within the interiors of stars fuse hydrogen to form helium. Therefore, helium is found inside many astrophysical objects, from planets, to stars, to white dwarf stars, and it plays a central role in their behavior. For example, recent experimental and theoretical work has shown that helium metallizes at terapascal pressures [10–12], which is higher than previously anticipated. As a consequence, it has been suggested that the cooling rate of white dwarf stars is slowed by their helium-rich atmospheres, and therefore current estimates of their ages need to be revised.

Helium has two electrons in the close-shell $1s$ state, and is chemically inert under ambient conditions. The only known helium compounds are either metastable, involving ionized species such as HeH_2^+ [17]; or are formed by weak van der Waals interactions, such as helium inside C_{60} [18]. Recently, a helium-sodium compound has been reported above pressures of about 0.1 TPa [19].

Iron has one of the highest binding energies per nucleon (the highest is ^{62}Ni) and is therefore also very abundant [20]. It accounts for about 80% of Earth's core mass [7], where it is found at pressures up to 0.35 TPa, and it is responsible for the magnetic field surrounding the planet [21]. Iron is not expected to exhibit magnetic order at terapascal pressures, and it is predicted to occur in a series of close-packed nonmagnetic crystal structures [22]. Iron compounds with hydrogen, carbon, oxygen, silicon, and sulfur have been investigated at pressures of about 0.35 TPa due to their importance for the composition of Earth's core [23].

In this Letter, we investigate the possibility that, under extreme compression, helium might form stable compounds with iron. The high abundances of helium and iron make it crucial to understand the helium-iron phase diagram for astrophysical modeling of the interiors of giant planets, including the increasing number of exoplanets being discovered [24], and iron-core white dwarf stars [25].

Our strategy is to search for high-pressure compounds of helium and iron using first-principles quantum mechanical density functional theory (DFT) methods as implemented in the CASTEP code [26], and the *ab initio* random structure searching (AIRSS) method [27]. The stability of a compound s with respect to the constituent elements can be evaluated by calculating the Gibbs free energy of formation per atom $\Delta\mathcal{G}_s = [\mathcal{G}_s - (\mathcal{G}_{He}N_{He} + \mathcal{G}_{Fe}N_{Fe})]/(N_{He} + N_{Fe})$, where $\mathcal{G}_s$ is the Gibbs free energy of the compound s, $\mathcal{G}_A$ is the Gibbs free energy per atom of A, and N_A is the number of A atoms in compound s. The Gibbs free energy has contributions from the electrons, which we calculate using DFT, and from the quantum and thermal nuclear motion, which we calculate using DFT within the harmonic approximation together with the recently proposed non-diagonal supercell approach [28] which greatly reduces the computational cost. Further details of the calculations are provided in the Supplemental Material [29].

We show the static lattice phase diagram of the helium-iron system in the pressure range 1–100 TPa in Fig. 1. Helium is predicted to adopt the hexagonal close-packed (hcp) crystal structure at TPa pressures [11]. Iron exhibits a sequence of phase transitions at terapascal pressures, starting with the hcp structure which transforms to the face-centered cubic (fcc) structure in the range 7–22 TPa, then it transforms back to the hcp structure up to pressures of 35 TPa, above which it transforms into the body-centered tetragonal (bct) structure, which approaches the body-centered cubic (bcc) structure with increasing pressure [22,33].

The structure searches find several compounds of helium and iron that are energetically competitive in the terapascal pressure range, and the most stable have stoichiometries FeHe and $FeHe_2$ (see Fig. 1). The FeHe stoichiometry first forms at 4 TPa in a structure of orthorhombic space group *Cmcm* containing eight atoms in the primitive cell, and at 50 TPa it transforms to a $Fm\bar{3}m$ structure (rocksalt structure). The $FeHe_2$ stoichiometry appears in three distinct structures which have similar energies. The first is an orthorhombic structure of space group *Cmmm* with nine atoms in the primitive cell, which forms around 12 TPa. The second has a space group of $I4_1/amd$ symmetry with six atoms in the primitive cell, and becomes the most stable $FeHe_2$ structure above 47 TPa. The third has $P6/mmm$ space group and three atoms in the primitive cell, but is not thermodynamically stable. Structure files for all of the helium-iron compounds are provided as Supplemental Material [29].

The helium-iron compounds that form at the lowest pressures have the FeHe *Cmcm* and the $FeHe_2$ *Cmmm* structures shown in Fig. 2. The iron atoms form open channels containing helium chains in the FeHe *Cmcm* structure [Fig. 2(a)]. At 10 TPa, the minimum He-He distance is 0.98 Å, the He-Fe distance is 1.16 Å, and the Fe-Fe distance is 1.47 Å. The volume per formula unit in FeHe is 2.76 Å^3, compared to 0.50 Å^3 in hcp helium and 2.27 Å^3 in both hcp and fcc iron, which add to a combined volume of 2.77 Å^3 per formula unit. In the $FeHe_2$ *Cmmm* structure [Fig. 2(b)], the helium atoms form hexagonal layers incorporated inside iron channels that are wider than those present in FeHe. The minimum He-He distance is 0.89 Å at 10 TPa, the He-Fe distance is 1.19 Å, and the Fe-Fe distance is larger at 1.54 Å. The volume per formula unit in $FeHe_2$ is 3.24 Å^3, which is smaller than that of the elements (total of 3.27 Å^3). The smaller volumes of the compounds favour their formation under pressure via the enthalpy term in the Gibbs free energy.

We next investigate the effects of temperature on the formation of helium-iron compounds upon increasing pressure. If the effects of nuclear motion are neglected, FeHe forms at pressures above 4.1 TPa, and the inclusion of quantum and thermal nuclear motion lowers this pressure to 2.7 TPa at 10 000 K. $FeHe_2$ only forms at a higher pressure of about 12 TPa, and therefore we focus on the FeHe compound to study the formation of helium-iron compounds under pressure.
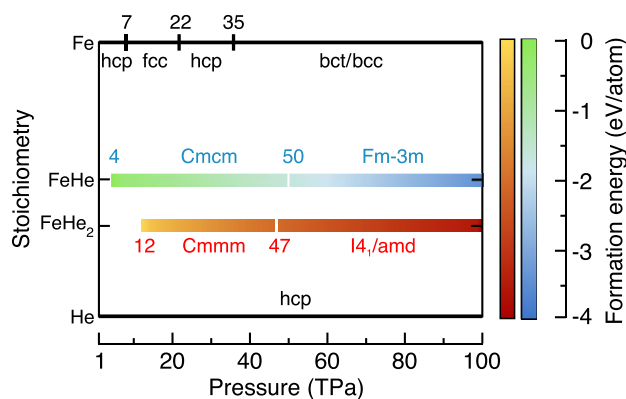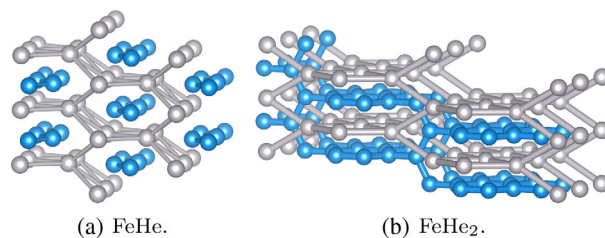

FIG. 1. Pressure-composition phase diagram of the helium-iron system at the static lattice level. For FeHe, the *Cmcm* structure is stable between 4 and 50 TPa, and the $Fm\bar{3}m$ structure above 50 TPa. For $FeHe_2$, the *Cmmm* structure is stable between 12 and 47 TPa, and above that pressure the stable structure is $I4_1/amd$. The formation energy per atom, calculated using $\Delta\mathcal{G}_s = [\mathcal{G}_s - (\mathcal{G}_{He}N_{He} + \mathcal{G}_{Fe}N_{Fe})]/(N_{He} + N_{Fe})$ as described in the text, is indicated by the gradients and approaches -4 eV/atom for both stoichiometries at 100 TPa.

FIG. 2. Crystal structures of *Cmcm* FeHe and *Cmmm* $FeHe_2$ at 10 TPa. Helium atoms are represented in blue, and iron atoms in gray.

We use *ab initio* molecular dynamics simulations in conjunction with the Z method [34] to estimate the melting temperature of FeHe. These calculations are performed using the QUANTUM ESPRESSO package [35], and the details are provided in the Supplemental Material [29]. The melting temperatures of helium and iron differ by thousands of degrees, suggesting that FeHe might exhibit superionicity, that is, sublattice melting of the helium component while the iron atoms oscillate around their crystallographic positions. Superionicity has been discussed before [36], for example, in a lithium-based conductor at ambient pressure [37], and in the melting of ice and ammonia at extreme pressures [8]. Indeed, our molecular dynamics simulations demonstrate that, upon increasing temperature, the helium chains melt within the iron channels in FeHe before the iron channels themselves melt. Interestingly, metallic superionic compounds are uncommon [38], and FeHe provides a nice platform to further investigate their properties.

In Fig. 3 we show the proposed phase diagram for the formation of helium-iron compounds under pressures up to 10 TPa. At low pressures, helium and iron do not mix. Below about 4000 K at 1 TPa and 6000 K at 3 TPa, both materials are found in the solid state, but helium melts above this temperature. Iron only melts at much higher temperatures, of the order of 15 000 K [39]. Upon increasing pressure, helium and iron form a FeHe compound between 2 and 4 TPa, depending on the temperature. FeHe undergoes sublattice melting of the helium atoms at

temperatures between 13 000 and 18 000 K, depending on the pressure. The superionic phase is stable in a wide temperature and pressure range, and melting is completed at around 17 000 K at 4 TPa, and above 19 000 K at 10 TPa.

Our results suggest that the FeHe compound should form at the pressures accessible to dynamic compression experiments. Furthermore, the formation pressure of FeHe is predicted to be within the pressure range found at the core of Jupiter, with a core-mantle boundary pressure of 4.2 TPa and temperature of 20 000 K, and at the highest pressures found at the center of Saturn, with a core-mantle boundary pressure of 1 TPa [14,40]. The interiors of exoplanets with masses similar to or larger than that of Jupiter will also be subject to pressures higher than those required to form FeHe. This raises the possibility that helium is captured by iron within the interior of these planets, and potentially bound to other elements. The atmosphere of Saturn is indeed depleted of helium [41], and the capture of helium in compounds in its interior could contribute to this phenomenon. This could also affect the helium composition of the atmospheres of giant exoplanets. White dwarf stars are subject to more extreme conditions, with helium-rich atmospheres subject to tens of terapascals, and the interiors to even higher pressures. Because of cooling, white dwarf stars exhibit temperatures in the range from only a few thousand kelvin to hundreds of thousand of kelvin [42], raising the possibility that even the solid FeHe phases appear in these stars. The formation of helium compounds with other elements could alter the cooling rates of white dwarf stars, which are largely determined by the atmospheric composition, and as a consequence affect current estimates of their ages. Our results indicate that, in contrast to the inertness of helium at ambient pressure, accurate models of the composition of planets and stars should treat helium as a compound-forming element.

In conclusion, we have used first-principles methods to study the binary phase diagram of helium and iron. We have found that compounds can form at pressures of several terapascals, suggesting that they might be found inside giant (exo)planets and white dwarf stars. We have also predicted that the most stable FeHe compound exhibits a superionic phase with sublattice melting of the helium atoms within a wide range of temperatures and pressures. Overall, our results show that helium can form compounds at terapascal pressures.
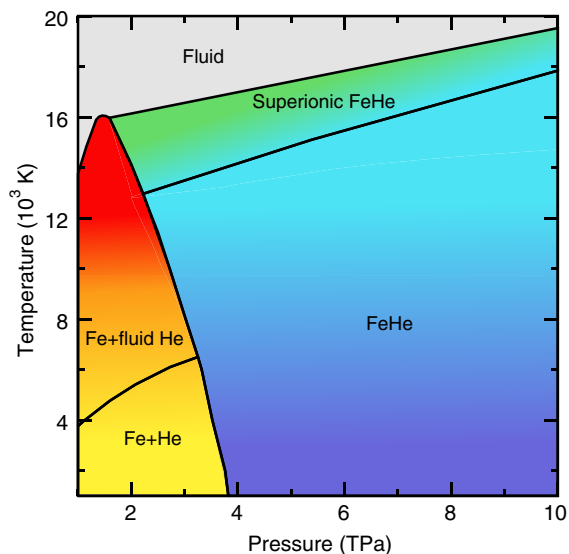

FIG. 3. Helium-iron phase diagram. The solid lines indicate formation lines, sublattice melting, and full melting. The sublattice melting of FeHe occurs at $15\,100 \pm 1000$ K at 5.38 TPa, and at $18\,200 \pm 1000$ K at 10.6 TPa, while the full melting of FeHe occurs at $17\,600 \pm 1000$ K at 5.45 TPa, and at $19\,800 \pm 1000$ K at 10.65 TPa. The melting line of iron is taken from Ref. [39].

---

*bm418@cam.ac.uk

[1] C. J. Pickard, M. Martinez-Canales, and R. J. Needs, Decomposition and Terapascal Phases of Water Ice, Phys. Rev. Lett. **110**, 245701 (2013).

[2] S. Ninet, F. Datchi, P. Dumas, M. Mezouar, G. Garbarino, A. Mafety, C. J. Pickard, R. J. Needs, and A. M. Saitta, Experimental and theoretical evidence for an ionic crystal of ammonia at high pressure, Phys. Rev. B **89**, 174103 (2014).

[3] D. Kobyakov and C. J. Pethick, Towards a Metallurgy of Neutron Star Crusts, Phys. Rev. Lett. **112**, 112504 (2014).

[4] A. P. Drozdov, M. I. Eremets, I. A. Troyan, V. Ksenofontov, and S. I. Shylin, Conventional superconductivity at 203 kelvin at high pressures in the sulfur hydride system, Nature (London) **525**, 73 (2015).

[5] D. Alfè, M. J. Gillan, and G. D. Price, The melting curve of iron at the pressures of the Earth's core from ab initio calculations, Nature (London) **401**, 462 (1999).

[6] M. Pozzo, C. Davies, D. Gubbins, and D. Alfè, Thermal and electrical conductivity of iron at Earth's core conditions, Nature (London) **485**, 355 (2012).

[7] C. Davies, M. Pozzo, D. Gubbins, and D. Alfè, Constraints from material properties on the dynamics and evolution of Earth's core, Nat. Geosci. **8**, 678 (2015).

[8] C. Cavazzoni, G. L. Chiarotti, S. Scandolo, E. Tosatti, M. Bernasconi, and M. Parrinello, Superionic and metallic states of water and ammonia at giant planet conditions, Science **283**, 44 (1999).

[9] H. F. Wilson, M. L. Wong, and B. Militzer, Superionic to Superionic Phase Change in Water: Consequences for the Interiors of Uranus and Neptune, Phys. Rev. Lett. **110**, 151102 (2013).

[10] S. A. Khairallah and B. Militzer, First-Principles Studies of the Metallization and the Equation of State of Solid Helium, Phys. Rev. Lett. **101**, 106407 (2008).

[11] B. Monserrat, N. D. Drummond, C. J. Pickard, and R. J. Needs, Electron-Phonon Coupling and the Metallization of Solid Helium at Terapascal Pressures, Phys. Rev. Lett. **112**, 055504 (2014).

[12] R. S. McWilliams, D. A. Dalton, Z. Konpkov, M. F. Mahmood, and A. F. Goncharov, Opacity and conductivity measurements in noble gases at conditions of planetary and stellar interiors, Proc. Natl. Acad. Sci. U.S.A. **112**, 7925 (2015).

[13] N. Dubrovinskaia, L. Dubrovinsky, N. A. Solopova, A. Abakumov, S. Turner, M. Hanfland, E. Bykova, M. Bykov, C. Prescher, V. B. Prakapenka, S. Petitgirard, I. Chuvashova, B. Gasharova, Y.-L. Mathis, P. Ershov, I. Snigireva, and A. Snigirev, Terapascal static pressure generation with ultrahigh yield strength nanodiamond, Sci. Adv. **2**, e1600341 (2016).

[14] W. B. Hubbard and B. Militzer, A preliminary Jupiter model, Astrophys. J. **820**, 80 (2016).

[15] R. F. Smith, J. H. Eggert, R. Jeanloz, T. S. Duffy, D. G. Braun, J. R. Patterson, R. E. Rudd, J. Biener, A. E. Lazicki, A. V. Hamza, J. Wang, T. Braun, L. X. Benedict, P. M. Celliers, and G. W. Collins, Ramp compression of diamond to five terapascals, Nature (London) **511**, 330 (2014).

[16] C. J. Pickard and R. J. Needs, High-pressure physics: Piling on the pressure, Nature (London) **511**, 294 (2014).

[17] T. R. Hogness and E. G. Lunn, The ionization of hydrogen by electron impact as interpreted by positive ray analysis, Phys. Rev. **26**, 44 (1925).

[18] M. Saunders, H. A. Jiménez-Vázquez, R. James Cross, and R. J. Poreda, Stable compounds of helium and neon: He@C60 and Ne@C60, Science **259**, 1428 (1993).

[19] X. Dong, A. R. Oganov, A. F. Goncharov, E. Stavrou, S. Lobanov, G. Saleh, G.-R. Qian, Q. Zhu, C. Gatti, V. L. Deringer, R. Dronskowski, X.-F. Zhou, V. B. Prakapenka, Z. Konôpková, I. A. Popov, A. I. Boldyrev, and H.-T. Wang, A stable compound of helium and sodium at high pressure, Nat. Chem. **9**, 440 (2017).

[20] E. M. Burbidge, G. R. Burbidge, W. A. Fowler, and F. Hoyle, Synthesis of the elements in stars, Rev. Mod. Phys. **29**, 547 (1957).

[21] B. A. Buffett, Earth's core and the geodynamo, Science **288**, 2007 (2000).

[22] C. J. Pickard and R. J. Needs, Stable phases of iron at terapascal pressures, J. Phys. Condens. Matter **21**, 452205 (2009).

[23] J.-P. Poirier, Light elements in the Earth's outer core: A critical review, Phys. Earth Planet. Inter. **85**, 319 (1994).

[24] M. Mayor, C. Lovis, and N. C. Santos, Doppler spectroscopy as a path to the detection of Earth-like planets, Nature (London) **513**, 328 (2014).

[25] G. C. Jordan IV, H. B. Perets, R. T. Fisher, and D. R. van Rossum, Failed-detonation supernovae: Subluminous low-velocity Ia supernovae and their kicked remnant white dwarfs with iron-rich cores, Astrophys. J. Lett. **761**, L23 (2012).

[26] S. J. Clark, M. D. Segall, C. J. Pickard, P. J. Hasnip, M. I. J. Probert, K. Refson, and M. C. Payne, First principles methods using CASTEP, Z. Kristallogr. **220**, 567 (2005).

[27] C. J. Pickard and R. J. Needs, Ab initio random structure searching, J. Phys. Condens. Matter **23**, 053201 (2011).

[28] J. H. Lloyd-Williams and B. Monserrat, Lattice dynamics and electron-phonon coupling calculations using nondiagonal supercells, Phys. Rev. B **92**, 184301 (2015).

[29] See Supplemental Material at http://link.aps.org/supplemental/10.1103/PhysRevLett.121.015301, which includes Refs. [30–32], for numerical details of the first-principles calculations and for cif files for the FeHe and $FeHe_2$ structures.

[30] J. P. Perdew, K. Burke, and M. Ernzerhof, Generalized Gradient Approximation Made Simple, Phys. Rev. Lett. **77**, 3865 (1996).

[31] C. J. Pickard and R. J. Needs, High-Pressure Phases of Silane, Phys. Rev. Lett. **97**, 045504 (2006).

[32] K. Kunc and R. M. Martin, Ab Initio force Constants of GaAs: A New Approach to Calculation of Phonons and Dielectric Properties, Phys. Rev. Lett. **48**, 406 (1982).

[33] L. Stixrude, Structure of Iron to 1 Gbar and 40 000 K, Phys. Rev. Lett. **108**, 055505 (2012).

[34] A. B. Belonoshko, N. V. Skorodumova, A. Rosengren, and B. Johansson, Melting and critical superheating, Phys. Rev. B **73,** 012201 (2006).

[35] P. Giannozzi, S. Baroni, N. Bonini, M. Calandra, R. Car, C. Cavazzoni, D. Ceresoli, G. L. Chiarotti, M. Cococcioni, I. Dabo *et al.*, QUANTUM ESPRESSO: A modular and open-source software project for quantum simulations of materials, J. Phys. Condens. Matter **21,** 395502 (2009).

[36] S. Hull, Superionics: Crystal structures and conduction processes, Rep. Prog. Phys. **67,** 1233 (2004).

[37] N. Kamaya, K. Homma, Y. Yamakawa, M. Hirayama, R. Kanno, M. Yonemura, T. Kamiyama, Y. Kato, S. Hama, K. Kawamoto, and A. Mitsui, A lithium superionic conductor, Nat. Mater. **10,** 682 (2011).

[38] M. French, T. R. Mattsson, and R. Redmer, Diffusion and electrical conductivity in water at ultrahigh pressures, Phys. Rev. B **82,** 174108 (2010).

[39] G. Morard, J. Bouchet, D. Valencia, S. Mazevet, and F. Guyot, The melting curve of iron at extreme pressures: Implications for planetary cores, High Energy Density Phys. **7,** 141 (2011).

[40] N. Nettelmann, A. Becker, B. Holst, and R. Redmer, Jupiter models with improved ab initio hydrogen equation of state (H-REOS.2), Astrophys. J. **750,** 52 (2012).

[41] D. J. Stevenson, Saturn's luminosity and magnetism, Science **208,** 746 (1980).

[42] B. M. S. Hansen and J. Liebert, Cool white dwarfs, Annu. Rev. Astron. Astrophys. **41,** 465 (2003).